Journal of the Mechanical Behavior of Biomedical Materials 72 (2017) 1–5

Contents lists available at ScienceDirect

Journal of the Mechanical Behavior of Biomedical Materials

journal homepage: www.elsevier.com/locate/jmbbm

Non-ideal effects in bending response of soft substrates covered with biomimetic scales

Ranajay Ghosh[a], Hamid Ebrahimi[b], Ashkan Vaziri[b,*]

[a] Department of Mechanical & Aerospace Engineering, University of Central Florida, Orlando, FL, United States
[b] Department of Mechanical and Industrial Engineering, Northeastern University, Boston, MA, United States

ARTICLE INFO

Keywords:
Biomimetic scales
Fish scales
Edge effects
Self-contact
Nonlinear response

ABSTRACT

Biomimetic scales are known to substantially alter the mechanics response of the underlying substrate engendering complex nonlinearities that can manifest even in small deformations due to scales interaction. This interaction is typically modeled using a-priori homogenization with an enforced periodicity of engagement. Such a framework is fairly useful especially when dealing with the structural length scale which is at least one order of magnitude greater than the scales themselves since individual tracking of a large number of scales become insurmountable. On the other hand, this scheme makes several assumptions whose validity has not yet been investigated including infinite length of the substrate and rigidity of the scales. The validity of these assumptions and the accuracy and limitations of associated analytical models are investigated. Finite element based numerical studies were carried out to identify the critical role of edge effects and other non-ideal behavior such as violation of periodicity and nonlinear constitutive response on scale rotation. Our investigation shows that several important quantities show a strong saturation characteristic which justify many of the simplifying assumptions whereas others need much greater care.

Matter and topology can both be used in conjunction to endow materials with highly non-traditional properties as evident in recently expanding research in metamaterials (Dimas et al., 2013; Dimas and Buehler, 2014; Ebrahimi et al., 2017; Haghpanah et al., 2016; Mousanezhad et al., 2015a, 2015b; Silverberg et al., 2014; Zhu et al., 2012). Such 'topological' strategies are also common in biological materials which are denuded of material choices. Topological organization can also boost multifunctionality to a great degree due to greater freedom in organization of material (Cowin, 2001; Gibson et al., 2010; Oftadeh et al., 2015). In this context, scales which are ubiquitous in animal kingdom are an ideal template for study. They are highly variegated and yet universal exhibiting a wide array of material properties, geometrical shapes and functions (Bruet et al., 2008; Ghiradella, 1991; Huang et al., 2006; Naleway et al., 2016; Yang et al., 2015; Zimmermann et al., 2013). Therefore, investigating materials which mimic the overall strategy of scaly surfaces can provide us with an important avenue of materials research.

Substrates with biomimetic scales demonstrate a classic biological strategy of structural and functional enhancements using topology of material organization (Li et al., 2015; Martini and Barthelat, 2016a, 2016b; Rudykh et al., 2015). This leverage partly relies on modulating the mechanics of deformation using intricate self-contact of scales driven by the geometry of the deforming structure (Ghosh et al., 2014; Vernerey and Barthelat, 2010, 2014). The difference in scales engagement geometry which depends on the curvature of the substrate, dictates the contact behavior kinematics of the scales as shown in Fig. 1(a). Here, a lab-scale sample of biomimetic scaly substrate was constructed using two polymers of highly contrasting stiffness such as Vinylpolysiloxane(VPS) and Acrylonitrile Butadiene Styrene (ABS) with the stiffer material used as scale and the softer as substrate material. This scales self-contact can substantially change the bending characteristic of the biomimetic substrate with enhanced stiffness even in small deformations, Fig. 1(b).

This general paradigm to introduce reversible stiffness gains has been studied in several recent studies which demonstrated the potential of biomimetic scales as high performance modern materials (Funk et al., 2015; Martini and Barthelat, 2016a; Wang et al., 2016; Yang et al., 2014). Specifically, this high contrast (materials with widely different stiffness) archetypical system has been modeled using a rigidity assumption on the scale and a linear elastic assumption for the substrate in the past (Ghosh et al., 2014, 2016). Although seemingly simple, using direct numerical simulation such as using finite elements (FE) to probe the behavior of more complicated scales distribution and geometry even for simple material behavior is prohibitively expensive especially for more densely packed scales. Therefore, investigations till date have used FE for less densely packed scales and homogenization

* Corresponding author.

http://dx.doi.org/10.1016/j.jmbbm.2017.04.019
Received 31 January 2017; Received in revised form 11 April 2017; Accepted 14 April 2017
Available online 15 April 2017

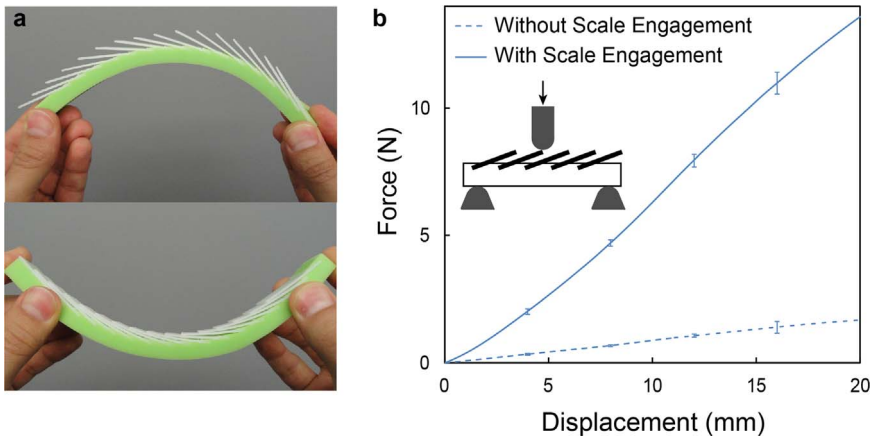

Fig. 1. (a) A manual illustration of the system deformation under bending in two opposite directions. (b) Comparative force response of biomimetic substrate-scale system and substrate with no scale under three-point bending experiment. (Adopted from Ghosh et al. APL (2014)).

for more densely packed regime invoking an implicit continuum level averaging of scales behavior with the imposition of strong periodicity. This periodicity provides a classical representative volume element (RVE), a natural averaging unit for material behavior. These idealized frameworks have improved our understanding of the most fundamental mechanisms of nonlinear behavior as well as revealed quantitative broad contours of performance of biomimetic scales (Browning et al., 2013; Ghosh et al., 2014, 2016; Vernerey and Barthelat, 2014; Vernerey et al., 2014).

However, these simplifying assumptions themselves have not been tested for limits of applicability for simple realistic imperfections. Understanding the effect of such imperfections would provide greater confidence in extending these models to more complex systems and also introduce empirical design parameters for extending purely theoretical models. The first step in that direction entails the determination of the limits of simplifications of the existing models to ascertain their extension. In this paper, we carry out extensive numerical studies to highlight the effectiveness and limitations of the simplifying assumptions typically employed in the high contrast biomimetic substrates (Ghosh et al., 2014) and set the stage for future more complex numerical and semi-analytical models for a more expansive biomimetic scaly substrates design.

At a broad level, using the regularity of scales engagement, modeling of local and global bending modes has traditionally relied on extracting performance characteristics through closed form relationships using a combination of elasticity, homogenization and imposition of periodicity (Ghosh et al., 2014, 2016; Vernerey and Barthelat, 2010, 2014; Vernerey et al., 2014) which leads to a classical representative volume element (RVE), a unit of averaging (Ghosh et al., 2014), Fig. 2.

The elasticity of the scales manifests itself in two different ways. First, elastic energy is absorbed by the substrate itself and thereafter additionally from the rotation of the scales themselves if the scales are sufficiently stiff neglecting their own deformation. Assuming linear elasticity for the substrate and rigidity for the highly stiff scale, the effect of scales rotation is often modeled as a torsional linear spring characterized by a fixed spring constant (Ghosh et al., 2014; Vernerey and Barthelat, 2010). A closed form expression for the torsional spring constant can be found by assuming that individual scales are well isolated from the adjacent scales (dilute scale distribution) as well as from the boundaries (remote scale location). At this point, imposing rigidity on the scale, the spring constant can be shown follow the analytical relationship (Ghosh et al., 2014) $K_{B,Ideal} = C_B E_B D^2 (\frac{L}{D})^n$ where E_B is the young's modulus of the base, D is the thickness of the scale and L is the embedded length of the scale, Fig. 3a (inset) and C_B,n are constants. Using an elastic system consisting of a very large substrate with a rigid prismatic body embedded in it simulates the remoteness and dilution of scales distribution. Extensive parametric FE simulations on this system yielded a very close fit for $L/D>10$ with $C_B \approx 0.66$. ,$n = 1.75$ (Ghosh et al., 2014).

However, in a non-ideal case, the thickness of the substrate is often only a few times more than the embedded length of the scales L which can influence the remoteness assumption. To this end, we define an index of deviation $\phi_h = \log (K^h_{B,NonIdeal}/K_{B,Ideal})$ where $K^h_{B,NonIdeal} = K_{B,NonIdeal}(h)$ is the FE computed stiffness for different values of normalized substrate thickness h/L whereas the width of the substrate is taken to be sufficiently large (dilute). In the FE models, rigid body constraint was imposed on the scales and two dimensional plain strain elements with sufficient mesh density was employed to achieve convergence. Substrate was clamped at the bottom and free at sides while a linear elastic material of E_{base}=2e4 *Pa* was assigned to the substrate. Initial angle of scale was 90° and rotation was applied on the scale at surface of the substrate and then exerted reaction moment was read to calculate K_B. The results plotted in Fig. 3(a) for various embedding aspect ratios L/D show a very strong deviation even when the substrate thickness is a

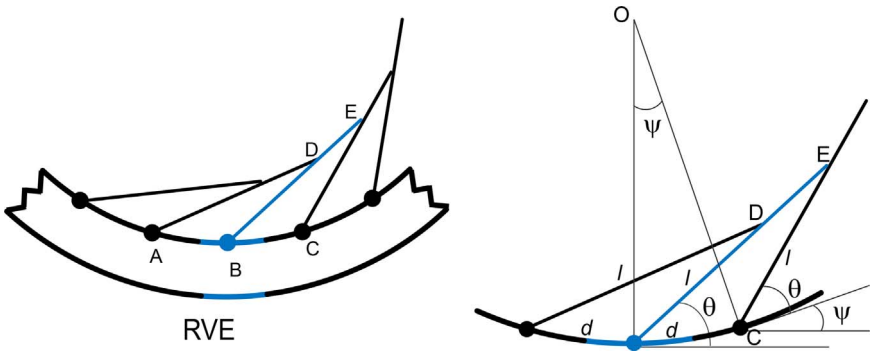

Fig. 2. RVE geometry of the biomimetic structure under bending load. (Adopted from Ghosh et al. APL (2014)).

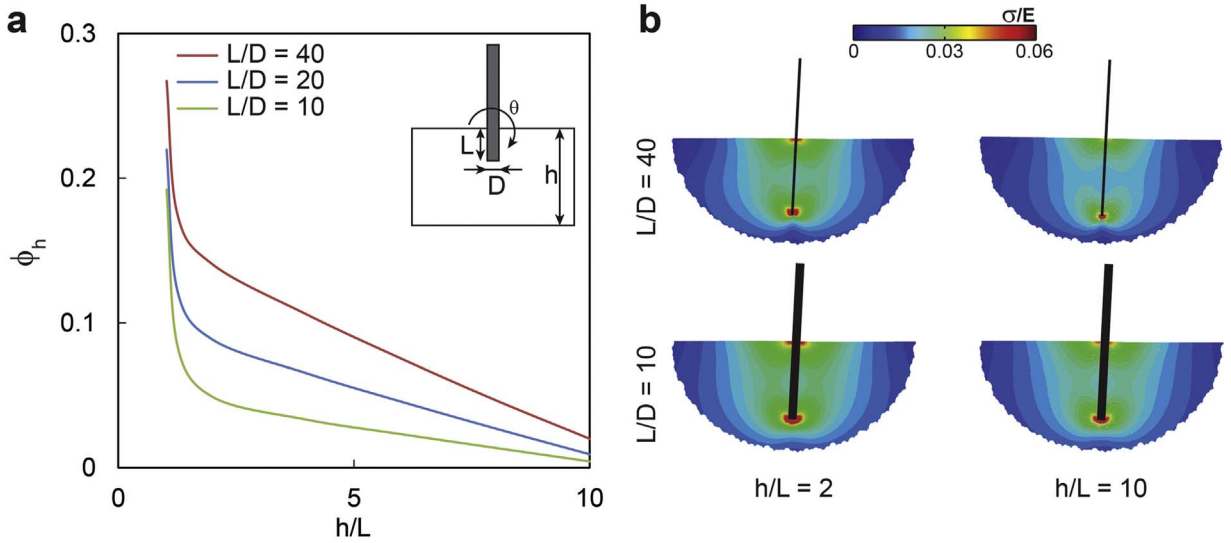

Fig. 3. (a) Saturating characteristic of rotational stiffness of the scales-substrate interaction (b) Comparison of von-Mises stress distribution to show stress concentration for h/L = 2 and 10 for two different values of L/D. The stress distributions are shown at θ = 0.05 rad.

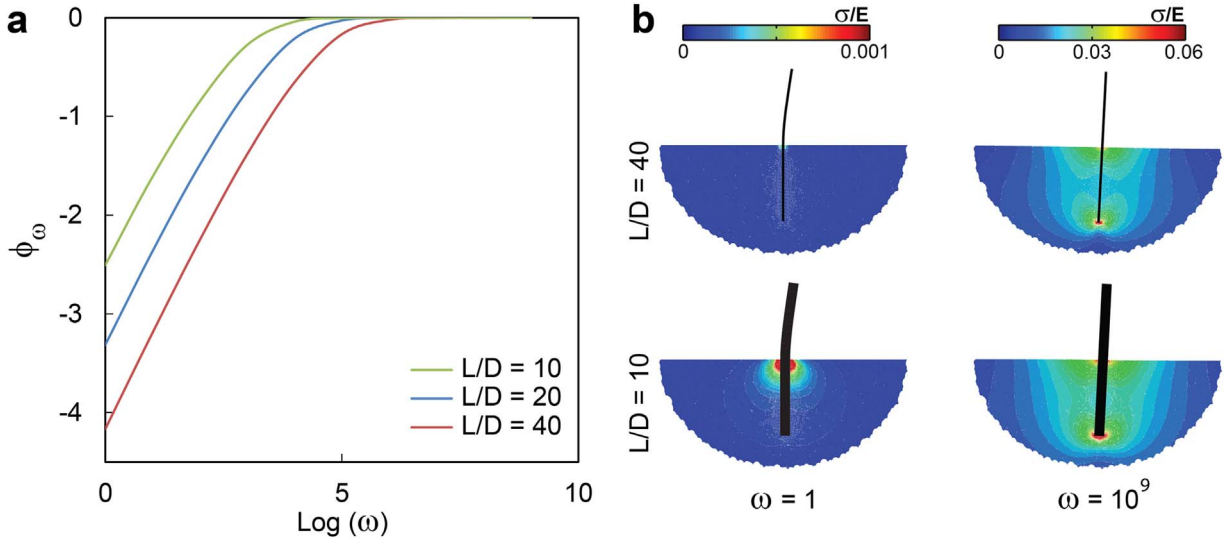

Fig. 4. (a) Saturating characteristic of rotational stiffness of the scales-substrate interaction versus Young's modulus ration of scale to substrate for h/L = 10. The figures spans from ω = 1 (i.e. scale and substrate have materials with same Young's modulus) to $\omega=10^9$. (b) Von-Mises stress distribution shows stress concentration for $\log(\omega) = 0$ and 9 at θ = 0.05 rad.

few times the embedding length. ϕ_h, which shows deviation from the ideal case, then begins to taper off substantially for all embedding aspect ratios as we increase the h/L ratio. Interestingly, the saturation characteristic is similar for both thicker and thinner scales for any given embedded length showing little influence of boundary effects on these scales as the thickness increases. This similarity of saturation is reflected in the similarity of von-Mises stress profile evolution with the relative thickness for two models with different L/D ratio cases as shown in Fig. 3(b). However, it is interesting that's despite the similarity in the overall trends with thickness primarily due to high contrast in Young's modulus between the scale and the substrate, the absolute value of deviation is higher for thinner scales when the substrates are substantially thinner. This indicates that the rotational stiffness scaling law is substantially poor approximation for thinner scales when the substrate thickness is lower. Therefore, we discover two competing effects on the accuracy of the model. Decreasing the thickness of the scale make it farther apart from boundary, improving the scaling law which assumes solitary scale embedded on an infinite medium, and at the same time, it potentially weakens it by making the model more sensitive to the remoteness assumption.

A further source of inaccuracy in the rotational stiffness relationship can arise due to the rigidity assumption of the scale. In order to ascertain this effect we plot the variation in FE computed non-ideal non-dimensional torsional constant, $\phi_\omega = \log\left(K^{\omega}_{B,NonIdeal}/K^{Rigid}_{B,NonIdeal}\right)$ against $\log\left(\omega=E_{scale}/E_{base}\right)$ where E_{Scale} is scale Young's modulus for three different L/D ratios, Fig. 4(a). Boundary conditions were same as previous case and substrate has linear elastic material of E_{base}=2e4 *Pa* while scales have linear elastic material with varying elastic modulus. We find as expected that the torsional spring constant increase by increasing in the scale stiffness by several orders of magnitude from $\omega = 1$ (i.e. same Young's modulus for scale and substrate) to $\log(\omega) = 9$. These results show that the rigidity assumption for scale plausible for the cases that scale made of material with more than six order of magnitude stiffer than the substrate. The difference in saturation characteristics for different L/D ratios is primarily due to the higher stress concentration for thicker scale as shown by the von-Mises stress contours in Fig. 4(b). Please note the different scale for stress distribution for different values of ω in this figure. The similarity of the stress contour for $\log(\omega) = 9$ with those in Fig. 3(b) also indicates the saturation effect and validity of assumption for scales that are stiffer enough than the substrate.

The above discussion highlights the non-ideal effects due to the

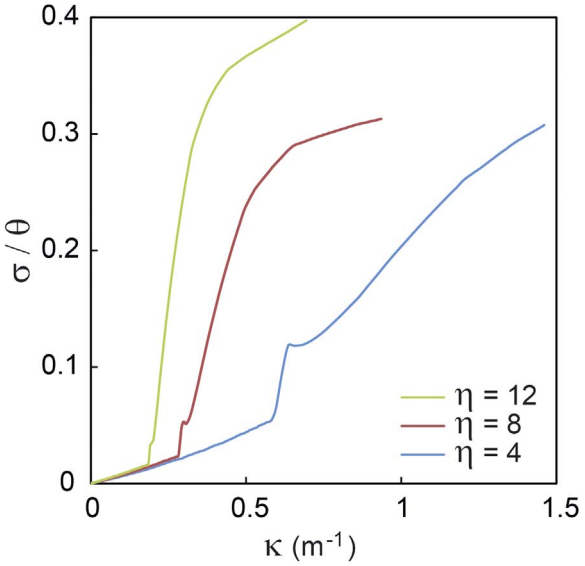

Fig. 5. Normalized deviation of the scale rotation from theoretical prediction versus bending curvature of the substrate, κ for three different values of $\eta = 4,8,$ *and*12 for $N = 48$.

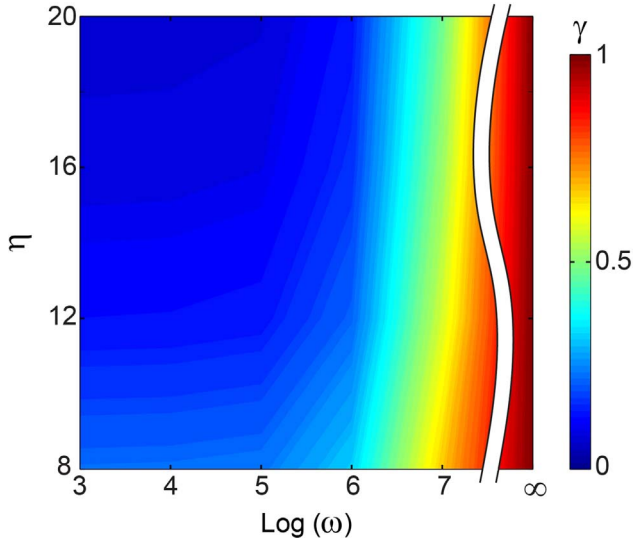

Fig. 7. Variation of the relative rigidity at engagement for the case of non-rigid scale normalized by the rigid assumption results, γ, spanned over overlap ratio, η and stiffness ratio of scale and substrate ratio, η and absolute number of scales.

geometry and compliance of the scales. However, recall that the mechanical nonlinearity of these substrates arises from the scales engagement kinematics in spite of all the idealizing assumptions. However, predicting this nonlinearity can turn out to be a very difficult problem for a general case. In spite of this, an immediate simplification is typically affected by assuming a periodic engagement of scales. Imposing periodicity as shown in Fig. 2, the following closed form nonlinear relationship was obtained between the scales rotation θ and substrate rotation per scale $\psi = \kappa d$ where κ is the bending curvature and d is the spacing between the scales (Ghosh et al., 2014):

$$\frac{\eta\psi \sin\theta - (1-\cos\psi)}{\eta\psi \cos\theta - \sin\psi} - \tan(\theta + \psi) = 0$$

with $\eta = l/d$ where l is the length of the scale. However, it is pertinent to investigate this assumption in somewhat more detail since any future multiscale homogenizations would tremendously benefit from at least a local periodicity of contacts resulting in the existence of an RVE. To this end, using finite element (FE) analysis we compute the accuracy of this assumption using an engagement index which is the mean of the angular deviation from predicted angle with both scale rotation and curvature for three different η, Fig. 5. We define this deviation as $\sigma = \sqrt{\frac{1}{N}\sum_{i=1}^{N}(\theta_i - \theta_{theo})^2}$ where θ_i is the rotation of *i-th* scale and N is the absolute number of scales in FE model. General contact formulation available in ABAQUS was employed to model contact of the scales with frictionless contact option. We discover that as the engagement proceeds, the deviation of periodicity begins to be worsens in a nonlinear fashion. The deviation at lower η is greater for initial stages of engagement. However, this trend reverses itself as the rotation proceeds with higher values of η exhibiting higher deviations. Interestingly, higher η tends to stabilize the deviation from periodicity at a much earlier stage of engagement.

In addition, to periodicity, the RVE level homogenization also needs a sufficiently large number of scales to approach the theoretical homogenized limit of predictions which must be RVE length scale independent. This limit can affect a number of pertinent variable that arise in the homogenized moment-curvature relationship. Among them, an important post engagement variable is the bending rigidity at

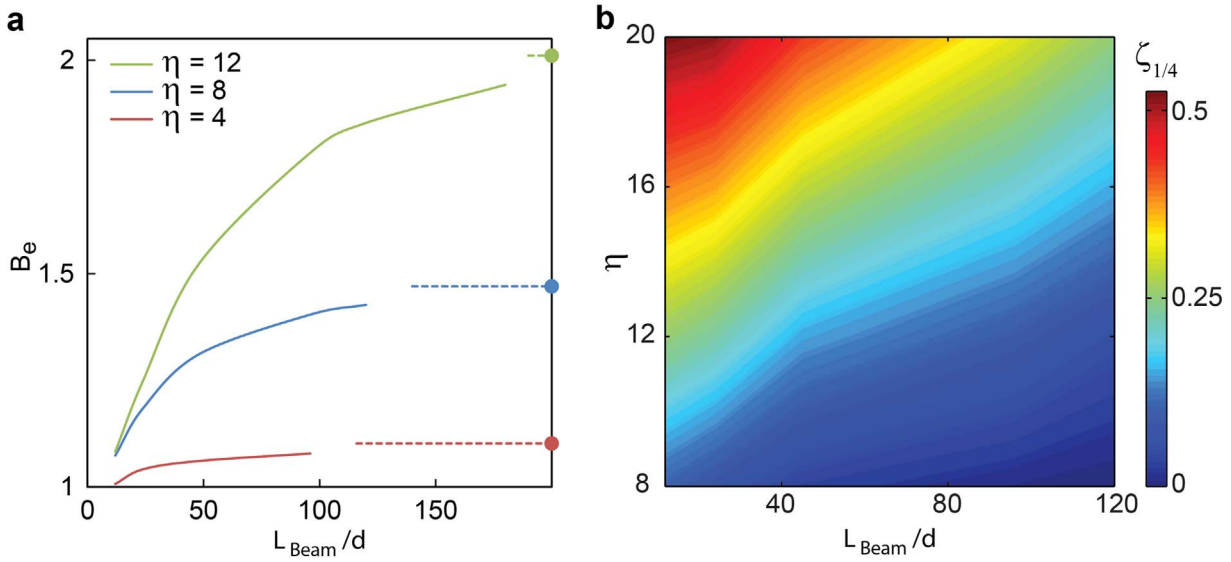

Fig. 6. (a) Variation of the relative rigidity at engagement, B_e, with the absolute number of scales. The dotted lines show theoretical prediction based on infinity assumption. (b) Relative additional elastic energy density of the biomimetic structure at ¼ the locking curvature spanned over overlap ratio, η and absolute number of scales.

engagement. This is computed by taking the slope of the FE computed moment curvature relationship at the point of engagement (B_e). This quantity serves as the lower bound of stiffness gained due to the biomimetic scales arrangement. Once again, using FE computed plots we show in Fig. 6(a), that shows B_e versus absolute number of scales for three different overlap ratios, it is clear that there is significant sensitivity to the number of scales. This sensitivity also depends on the overlap ratio η. In general, as expected, a saturating relationship is observed with the number of scales (RVE number). However, the saturation is far slower than those printed on typical lab samples especially for higher η. Therefore, the theoretical predictions can significantly overestimate the stiffness gains when the scales are lower in number. This can be an important design parameter for these systems. We also quantify the RVE number dependence well into engagement. Thus, we define relative additional elastic energy density at quarter locking curvature $\left(\zeta_{1/4} = \frac{|E_{theo} - E_{comp}|}{E_{theo}} |_{\kappa=\kappa_{lock}/4}\right)$ with the absolute number of scales. We plot this variation of FE computed additional elastic energy of engagement at quarter locking curvature Fig. 6(b). As expected this figure also shows a strongly saturating characteristic with scale numbers.

Note that the bending characteristics would also be affected by the scale compliance both due to deviation from the theoretical torsional stiffness computed earlier as well as from the rigid material assumption of the scale. We further quantify this aspect of non-ideal behavior of the bending characteristic using the familiar bending rigidity at engagement ratio through a non-dimensional index $\gamma = B_e^{\omega}/B_e^{Rigid}$ where B_e^{Rigid} shows the FE computed bending rigidity at engagement for the case of rigid scale and, which would be mapped via two other pertinent non-dimensional numbers $\omega = E_{scale}/E_{base}$, which quantifies the relative stiffness contrast of the base and the scale, and η, Fig. 7. The figure indicates that at least six orders of magnitude difference between the scale and substrate is needed to justify the rigidity assumption.

In conclusion, we carried out a detailed exposition of non-ideal limits of geometry and materials on the previous models of biomimetic scales engagement. Such limits are essential when extending the models to the cases of multiscale modeling and homogenized media. By finding specific limits of applicability of models, we find that several of the assumptions hold strongly whereas some others are subject to severe limitations. Specifically we find that the ratio of the substrate height to the embedded length of the scale cause strong deviation from the theoretical prediction of the mechanical response within the typical range. This is one the major sources of the limitation of applying theoretical investigation into actual designs. Rigidity assumption holds true in calculation of spring constant of an individual scale for a fairly stiff scale with respect to substrate however it's effect is more profound for the bending rigidity of the scale-substrate system where scale needs to be more than eight order of magnitude stiffer than the substrate for the results to be within 90% of the theoretical value. The last important limitation factor was the length of the substrate (absolute number of scales). There is clearly a saturation effect in the behavior of the system with respect to absolute number of scales, however, one need less number of scales to get reasonably close to predicted value for smaller overlap ratio than for the larger values of η. This study reveals the range of geometrical and material properties that assumptions for theoretical investigation hold true and can be used in designing high performance modern materials.

Acknowledgement

This work was supported by the United States National Science Foundation's Civil, Mechanical, and Manufacturing Innovation Grant No. 1149750.

References

Browning, A., Ortiz, C., Boyce, M.C., 2013. Mechanics of composite elasmoid fish scale assemblies and their bioinspired analogues. J. Mech. Behav. Biomed. Mater. 19, 75–86.
Bruet, B.J.F., Song, J., Boyce, M.C., Ortiz, C., 2008. Materials design principles of ancient fish armour. Nat. Mater. 7, 748–756.
Cowin, S.C., 2001. Bone Mechanics Handbook. CRC press.
Dimas, L.S., Bratzel, G.H., Eylon, I., Buehler, M.J., 2013. Tough composites inspired by mineralized natural materials: computation, 3D printing, and testing. Adv. Funct. Mater. 23, 4629–4638.
Dimas, L.S., Buehler, M.J., 2014. Modeling and additive manufacturing of bio-inspired composites with tunable fracture mechanical properties. Soft Matter 10, 4436–4442.
Ebrahimi, H., Mousanezhad, D., Haghpanah, B., Ghosh, R., Vaziri, A., 2017. Lattice materials with reversible foldability. Adv. Eng. Mater. 19 (2), 1600646.
Funk, N., Vera, M., Szewciw, L.J., Barthelat, F., Stoykovich, M.P., Vernerey, F.J., 2015. Bioinspired fabrication and characterization of a synthetic fish skin for the protection of soft materials. ACS Appl. Mater. Interfaces 7, 5972–5983.
Ghiradella, H., 1991. Light and color on the wing: structural colors in butterflies and moths. Appl. Opt. 30, 3492–3500.
Ghosh, R., Ebrahimi, H., Vaziri, A., 2014. Contact kinematics of biomimetic scales. Appl. Phys. Lett. 105, 233701.
Ghosh, R., Ebrahimi, H., Vaziri, A., 2016. Frictional effects in biomimetic scales engagement. Eurphys. Lett. 113, 34003.
Gibson, L.J., Ashby, M.F., Harley, B.A., 2010. Cellular Materials in Nature and Medicine. Cambridge University Press.
Haghpanah, B., Salari-Sharif, L., Pourrajab, P., Hopkins, J., Valdevit, L., 2016. Multistable shape-reconfigurable architected materials. Adv. Mater. 28, 7915–7920.
Huang, J., Wang, X., Wang, Z.L., 2006. Controlled replication of butterfly wings for achieving tunable photonic properties. Nano Lett. 6, 2325–2331.
Li, W., James, C.W., Patrick, J.M.T., George, V.L., 2015. Hydrodynamic function of biomimetic shark skin: effect of denticle pattern and spacing. Bioinspir. Biomim. 10, 066010.
Martini, R., Barthelat, F., 2016a. Stability of hard plates on soft substrates and application to the design of bioinspired segmented armor. J. Mech. Phys. Solids 92, 195–209.
Martini, R., Barthelat, F., 2016b. Stretch-and-release fabrication, testing and optimization of a flexible ceramic armor inspired from fish scales. Bioinspir. Biomim. 11, 066001.
Mousanezhad, D., Babaee, S., Ebrahimi, H., Ghosh, R., Hamouda, A.S., Bertoldi, K., Vaziri, A., 2015a. Hierarchical honeycomb auxetic metamaterials. Sci. Rep. 5, 18306.
Mousanezhad, D., Ebrahimi, H., Haghpanah, B., Ghosh, R., Ajdari, A., Hamouda, A.M.S., Vaziri, A., 2015b. Spiderweb honeycombs. Int. J Solids Struct. 66, 218–227.
Naleway, S.E., Taylor, J.R.A., Porter, M.M., Meyers, M.A., McKittrick, J., 2016. Structure and mechanical properties of selected protective systems in marine organisms. Mater. Sci. Eng.: C 59, 1143–1167.
Oftadeh, R., Perez-Viloria, M., Villa-Camacho, J.C., Vaziri, A., Nazarian, A., 2015. Biomechanics and mechanobiology of trabecular bone: a review. J. Biomech. Eng. 137 [010802-010802-010815].
Rudykh, S., Ortiz, C., Boyce, M.C., 2015. Flexibility and protection by design: imbricated hybrid microstructures of bio-inspired armor. Soft Matter 11, 2547–2554.
Silverberg, J.L., Evans, A.A., McLeod, L., Hayward, R.C., Hull, T., Santangelo, C.D., Cohen, I., 2014. Using origami design principles to fold reprogrammable mechanical metamaterials. Science 345, 647–650.
Vernerey, F.J., Barthelat, F., 2010. On the mechanics of fishscale structures. Int. J Solids Struct. 47, 2268–2275.
Vernerey, F.J., Barthelat, F., 2014. Skin and scales of teleost fish: simple structure but high performance and multiple functions. J. Mech. Phys. Solids 68, 66–76.
Vernerey, F.J., Musiket, K., Barthelat, F., 2014. Mechanics of fish skin: a computational approach for bio-inspired flexible composites. Int. J Solids Struct. 51, 274–283.
Wang, B., Yang, W., Sherman, V.R., Meyers, M.A., 2016. Pangolin armor: overlapping, structure, and mechanical properties of the keratinous scales. Acta Biomater. 41, 60–74.
Yang, W., Naleway, S.E., Porter, M.M., Meyers, M.A., McKittrick, J., 2015. The armored carapace of the boxfish. Acta Biomater. 23, 1–10.
Yang, W., Sherman, V.R., Gludovatz, B., Mackey, M., Zimmermann, E.A., Chang, E.H., Schaible, E., Qin, Z., Buehler, M.J., Ritchie, R.O., Meyers, M.A., 2014. Protective role of Arapaima gigas fish scales: structure and mechanical behavior. Acta Biomater. 10, 3599–3614.
Zhu, D., Ortega, C.F., Motamedi, R., Szewciw, L., Vernerey, F., Barthelat, F., 2012. Structure and mechanical performance of a “Modern” fish scale. Adv. Eng. Mater. 14, B185–B194.
Zimmermann, E.A., Gludovatz, B., Schaible, E., Dave, N.K.N., Yang, W., Meyers, M.A., Ritchie, R.O., 2013. Mechanical adaptability of the Bouligand-type structure in natural dermal armour. Nat. Commun. 4, 2634.